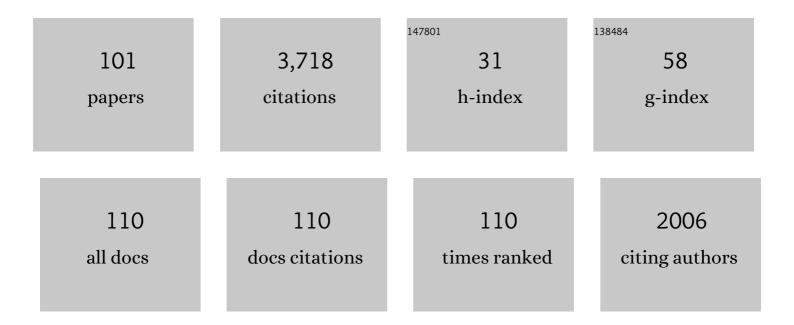
Mauro Ciarniello

List of Publications by Year in descending order

Source: https://exaly.com/author-pdf/5983660/publications.pdf Version: 2024-02-01



MALIPO CIADNIELLO

#	Article	IF	CITATIONS
1	The organic-rich surface of comet 67P/Churyumov-Gerasimenko as seen by VIRTIS/Rosetta. Science, 2015, 347, aaa0628.	12.6	293
2	Ammoniated phyllosilicates with a likely outer Solar System origin on (1) Ceres. Nature, 2015, 528, 241-244.	27.8	276
3	Bright carbonate deposits as evidence of aqueous alteration on (1) Ceres. Nature, 2016, 536, 54-57.	27.8	240
4	The diurnal cycle of water ice on comet 67P/Churyumov–Gerasimenko. Nature, 2015, 525, 500-503.	27.8	199
5	Distribution of phyllosilicates on the surface of Ceres. Science, 2016, 353, .	12.6	159
6	Localized aliphatic organic material on the surface of Ceres. Science, 2017, 355, 719-722.	12.6	152
7	Refractory and semi-volatile organics at the surface of comet 67P/Churyumov-Gerasimenko: Insights from the VIRTIS/Rosetta imaging spectrometer. Icarus, 2016, 272, 32-47.	2.5	127
8	Ammonium salts are a reservoir of nitrogen on a cometary nucleus and possibly on some asteroids. Science, 2020, 367, .	12.6	115
9	Exposed water ice on the nucleus of comet 67P/Churyumov–Gerasimenko. Nature, 2016, 529, 368-372.	27.8	104
10	Saturn's icy satellites and rings investigated by Cassini–VIMS: III – Radial compositional variability. Icarus, 2012, 220, 1064-1096.	2.5	86
11	Nature, formation, and distribution of carbonates on Ceres. Science Advances, 2018, 4, e1701645.	10.3	83
12	Spectral analysis of Ahuna Mons from Dawn mission's visibleâ€infrared spectrometer. Geophysical Research Letters, 2017, 44, 97-104.	4.0	74
13	Photometric properties of comet 67P/Churyumov-Gerasimenko from VIRTIS-M onboard Rosetta. Astronomy and Astrophysics, 2015, 583, A31.	5.1	71
14	Resolved spectrophotometric properties of the Ceres surface from Dawn Framing Camera images. Icarus, 2017, 288, 201-225.	2.5	69
15	Spectrophotometric properties of dwarf planet Ceres from the VIR spectrometer on board the Dawn mission. Astronomy and Astrophysics, 2017, 598, A130.	5.1	69
16	Detection of exposed H ₂ O ice on the nucleus of comet 67P/Churyumov-Gerasimenko. Astronomy and Astrophysics, 2016, 595, A102.	5.1	67
17	Hapke modeling of Rhea surface properties through Cassini-VIMS spectra. Icarus, 2011, 214, 541-555.	2.5	64
18	Mineralogy of Occator crater on Ceres and insight into its evolution from the properties of carbonates, phyllosilicates, and chlorides. Icarus, 2019, 320, 83-96.	2.5	63

#	Article	IF	CITATIONS
19	An aqueously altered carbon-rich Ceres. Nature Astronomy, 2019, 3, 140-145.	10.1	62
20	Seasonal exposure of carbon dioxide ice on the nucleus of comet 67P/Churyumov-Gerasimenko. Science, 2016, 354, 1563-1566.	12.6	61
21	Fresh emplacement of hydrated sodium chloride on Ceres from ascending salty fluids. Nature Astronomy, 2020, 4, 786-793.	10.1	60
22	The global surface composition of 67P/CG nucleus by Rosetta/VIRTIS. (I) Prelanding mission phase. Icarus, 2016, 274, 334-349.	2.5	54
23	Spectral variability of plagioclase–mafic mixtures (1): Effects of chemistry and modal abundance in reflectance spectra of rocks and mineral mixtures. Icarus, 2013, 226, 282-298.	2.5	52
24	Variations in the amount of water ice on Ceres' surface suggest a seasonal water cycle. Science Advances, 2018, 4, eaao3757.	10.3	43
25	Infrared detection of aliphatic organics on a cometary nucleus. Nature Astronomy, 2020, 4, 500-505.	10.1	41
26	Connections between spectra and structure in Saturn's main rings based on Cassini VIMS data. Icarus, 2013, 223, 105-130.	2.5	40
27	The Philae lander reveals low-strength primitive ice inside cometary boulders. Nature, 2020, 586, 697-701.	27.8	40
28	An orbital water-ice cycle on comet 67P from colour changes. Nature, 2020, 578, 49-52.	27.8	36
29	The changing temperature of the nucleus of comet 67P induced by morphological and seasonal effects. Nature Astronomy, 2019, 3, 649-658.	10.1	34
30	Compositional differences among Bright Spots on the Ceres surface. Icarus, 2019, 320, 202-212.	2.5	33
31	Comet 67P/CG Nucleus Composition and Comparison to Other Comets. Space Science Reviews, 2019, 215, 1.	8.1	32
32	Spectral variability of plagioclase–mafic mixtures (2): Investigation of the optical constant and retrieved mineral abundance dependence on particle size distribution. Icarus, 2014, 235, 207-219.	2.5	30
33	Characteristics of organic matter on Ceres from VIR/Dawn high spatial resolution spectra. Monthly Notices of the Royal Astronomical Society, 2019, 482, 2407-2421.	4.4	30
34	Ceres's global and localized mineralogical composition determined by Dawn's Visible and Infrared Spectrometer (<scp>VIR</scp>). Meteoritics and Planetary Science, 2018, 53, 1844-1865.	1.6	29
35	THE RADIAL DISTRIBUTION OF WATER ICE AND CHROMOPHORES ACROSS SATURN'S SYSTEM. Astrophysical Journal, 2013, 766, 76.	4.5	26
36	Spectroscopic classification of icy satellites of Saturn II: Identification of terrain units on Rhea. Icarus, 2014, 234, 1-16.	2.5	26

#	Article	IF	CITATIONS
37	Cassini–VIMS observations of Saturn's main rings: I. Spectral properties and temperature radial profiles variability with phase angle and elevation. Icarus, 2014, 241, 45-65.	2.5	24
38	Close Cassini flybys of Saturn's ring moons Pan, Daphnis, Atlas, Pandora, and Epimetheus. Science, 2019, 364, .	12.6	24
39	Saturn's icy satellites investigated by Cassini-VIMS. IV. Daytime temperature maps. Icarus, 2016, 271, 292-313.	2.5	23
40	Laboratory simulations of the Vis-NIR spectra of comet 67P using sub-µm sized cosmochemical analogues. Icarus, 2018, 306, 306-318.	2.5	23
41	Spectroscopic classification of icy satellites of Saturn I: Identification of terrain units on Dione. Icarus, 2013, 226, 1331-1349.	2.5	22
42	A test of Hapke's model by means of Monte Carlo ray-tracing. Icarus, 2014, 237, 293-305.	2.5	22
43	How pristine is the interior of the comet 67P/Churyumov–Gerasimenko?. Monthly Notices of the Royal Astronomical Society, 2017, 469, S685-S694.	4.4	22
44	Mineralogy and temperature of crater Haulani on Ceres. Meteoritics and Planetary Science, 2018, 53, 1902-1924.	1.6	21
45	Spectrophotometric modeling and mapping of Ceres. Icarus, 2019, 322, 144-167.	2.5	21
46	Summer outbursts in the coma of comet 67P/Churyumov–Gerasimenko as observed by Rosetta–VIRTIS. Monthly Notices of the Royal Astronomical Society, 2018, 481, 1235-1250.	4.4	20
47	Mineralogical mapping of Coniraya quadrangle of the dwarf planet Ceres. Icarus, 2019, 318, 99-110.	2.5	20
48	Macro and micro structures of pebble-made cometary nuclei reconciled by seasonal evolution. Nature Astronomy, 2022, 6, 546-553.	10.1	20
49	Cassini-VIMS observations of Saturn's main rings: II. A spectrophotometric study by means of Monte Carlo ray-tracing and Hapke's theory. Icarus, 2019, 317, 242-265.	2.5	17
50	VIRTIS-H observations of the dust coma of comet 67P/Churyumov-Gerasimenko: spectral properties and color temperature variability with phase and elevation. Astronomy and Astrophysics, 2019, 630, A22.	5.1	17
51	Photometry of Ceres and Occator faculae as inferred from VIR/Dawn data. Icarus, 2019, 320, 97-109.	2.5	17
52	Photometric behaviour of 67P/Churyumov–Gerasimenko and analysis of its pre-perihelion diurnal variations. Monthly Notices of the Royal Astronomical Society, 2017, 469, S346-S356.	4.4	16
53	Infrared Observations of Ganymede From the Jovian InfraRed Auroral Mapper on Juno. Journal of Geophysical Research E: Planets, 2020, 125, e2020JE006508.	3.6	16
54	Serendipitous infrared observations of Europa by Juno/JIRAM. Icarus, 2019, 328, 1-13.	2.5	15

#	Article	IF	CITATIONS
55	67P/Churyumov–Gerasimenko's dust activity from pre- to post-perihelion as detected by Rosetta/GIADA. Monthly Notices of the Royal Astronomical Society, 2020, 496, 125-137.	4.4	15
56	The temporal evolution of exposed water ice-rich areas on the surface of 67P/Churyumov-Gerasimenko: spectral analysis. Monthly Notices of the Royal Astronomical Society, 0, , stw3281.	4.4	13
57	Cometary coma dust size distribution from in situ IR spectra. Monthly Notices of the Royal Astronomical Society, 2017, 469, S598-S605.	4.4	12
58	Organic Material on Ceres: Insights from Visible and Infrared Space Observations. Life, 2021, 11, 9.	2.4	12
59	Hydroxylated Mg-rich Amorphous Silicates: A New Component of the 3.2 μm Absorption Band of Comet 67P/Churyumov–Gerasimenko. Astrophysical Journal Letters, 2020, 897, L37.	8.3	12
60	Disk-resolved photometry of Vesta and Lutetia and comparison with other asteroids. Icarus, 2016, 267, 204-216.	2.5	11
61	Mineralogical analysis of the Ac-H-6 Haulani quadrangle of the dwarf planet Ceres. Icarus, 2019, 318, 170-187.	2.5	11
62	Mineralogy of the Occator quadrangle. Icarus, 2019, 318, 205-211.	2.5	11
63	A Probabilistic Approach to Determination of Ceres' Average Surface Composition From Dawn Visibleâ€Infrared Mapping Spectrometer and Gamma Ray and Neutron Detector Data. Journal of Geophysical Research E: Planets, 2020, 125, e2020JE006606.	3.6	11
64	and seasonal variability. Monthly Notices of the Royal Astronomical Society, 0, , stw3177.	4.4	10
65	Ceres' opposition effect observed by the Dawn framing camera. Astronomy and Astrophysics, 2018, 620, A201.	5.1	9
66	The spectral parameter maps of Ceres from NASA/DAWN VIR data. Icarus, 2019, 318, 14-21.	2.5	9
67	Diurnal variation of dust and gas production in comet 67P/Churyumov-Gerasimenko at the inbound equinox as seen by OSIRIS and VIRTIS-M on board Rosetta. Astronomy and Astrophysics, 2019, 630, A23.	5.1	9
68	Correction of the VIR-visible data set from the Dawn mission. Review of Scientific Instruments, 2019, 90, 123110.	1.3	9
69	Ac-H-11 Sintana and Ac-H-12 Toharu quadrangles: Assessing the large and small scale heterogeneities of Ceres' surface. Icarus, 2019, 318, 230-240.	2.5	9
70	High Thermal Inertia Zones on Ceres From Dawn Data. Journal of Geophysical Research E: Planets, 2020, 125, e2018JE005733.	3.6	9
71	The SSDC contribution to the improvement of knowledge by means of 3D data projections of minor bodies. Advances in Space Research, 2018, 62, 2306-2316.	2.6	8
72	Analysis of night-side dust activity on comet 67P observed by VIRTIS-M: a new method to constrain the thermal inertia on the surface. Astronomy and Astrophysics, 2019, 630, A21.	5.1	8

#	Article	IF	CITATIONS
73	67P/Churyumov–Gerasimenko active areas before perihelion identified by GIADA and VIRTIS data fusion. Monthly Notices of the Royal Astronomical Society, 2019, 483, 2165-2176.	4.4	8
74	Mineralogical analysis of quadrangle Ac-H-10 Rongo on the dwarf planet Ceres. Icarus, 2019, 318, 212-229.	2.5	8
75	Mineralogical mapping of the Kerwan quadrangle on Ceres. Icarus, 2019, 318, 188-194.	2.5	8
76	Mapping Io's Surface Composition With Juno/JIRAM. Journal of Geophysical Research E: Planets, 2020, 125, e2020JE006522.	3.6	8
77	Ceres observed at low phase angles by VIR-Dawn. Astronomy and Astrophysics, 2020, 634, A39.	5.1	8
78	The surface of (1) Ceres in visible light as seen by Dawn/VIR. Astronomy and Astrophysics, 2020, 642, A74.	5.1	8
79	Photometric Modeling and VISâ€IR Albedo Maps of Dione From Cassiniâ€VIMS. Geophysical Research Letters, 2018, 45, 2184-2192.	4.0	7
80	Continuum definition for â^1⁄43.1, â^1⁄43.4 and â^1⁄44.0 µm absorption bands in Ceres spectra and evaluation of effects of smoothing procedure in the retrieved spectral parameters. Advances in Space Research, 2018, 62, 2342-2354.	2.6	7
81	Bayesian analysis of Juno/JIRAM's NIR observations of Europa. Icarus, 2021, 357, 114215.	2.5	7
82	Photometric Modeling and VISâ€IR Albedo Maps of Tethys From Cassiniâ€VIMS. Geophysical Research Letters, 2018, 45, 6400-6407.	4.0	6
83	Mineralogy of the Urvara–Yalode region on Ceres. Icarus, 2019, 318, 241-250.	2.5	6
84	The surface composition of Ceres' Ezinu quadrangle analyzed by the Dawn mission. Icarus, 2019, 318, 124-146.	2.5	6
85	Highâ€Temperature VISâ€IR Spectroscopy of NH ₄ â€Phyllosilicates. Journal of Geophysical Research E: Planets, 2021, 126, e2020JE006696.	3.6	6
86	Laboratory Investigations Coupled to VIR/Dawn Observations to Quantify the Large Concentrations of Organic Matter on Ceres. Minerals (Basel, Switzerland), 2021, 11, 719.	2.0	6
87	VIS-NIR/SWIR Spectral Properties of H2O Ice Depending on Particle Size and Surface Temperature. Minerals (Basel, Switzerland), 2021, 11, 1328.	2.0	6
88	VIS-IR Spectroscopy of Mixtures of Water Ice, Organic Matter, and Opaque Mineral in Support of Small Body Remote Sensing Observations. Minerals (Basel, Switzerland), 2021, 11, 1222.	2.0	4
89	Photometric modelling and VIS-IR albedo maps of Rhea from Cassini-VIMS. Monthly Notices of the Royal Astronomical Society: Letters, 2020, 499, L62-L66.	3.3	3
90	Temporal evolution of the permanent shadowed regions at Mercury poles: applications for spectral detection of ices by SIMBIOSYS-VIHI on BepiColombo mission. Monthly Notices of the Royal Astronomical Society, 2020, 498, 1308-1318.	4.4	3

#	Article	IF	CITATIONS
91	Correction of the VIR-visible dataset from the Dawn mission at Vesta. Review of Scientific Instruments, 2020, 91, 123102.	1.3	3
92	Saturn's icy satellites investigated by Cassini - VIMS. V. Spectrophotometry. Icarus, 2022, 375, 114803.	2.5	3
93	Iron rich basaltic eucrites, implication on spectral properties and parental bodies. Icarus, 2022, 371, 114653.	2.5	2
94	MINERALOGICAL MAPPING OF THE OCCATOR QUADRANGLE. , 2016, , .		2
95	The mineralogy of Ceres' Nawish quadrangle. Icarus, 2019, 318, 195-204.	2.5	1
96	Mineralogy mapping of the Ac-H-5 Fejokoo quadrangle of Ceres. Icarus, 2019, 318, 147-169.	2.5	1
97	Saturn System. , 2021, , 123-132.		1
98	The surface of (4) Vesta in visible light as seen by Dawn/VIR. Astronomy and Astrophysics, 2021, 653, A118.	5.1	1
99	MINERALOGICAL ANALYSIS OF THE QUADRANGLES AC-11 SINTANA AND AC-12 TOHARU ON THE DWARF PLANET CERES. , 2016, , .		1
100	Spectroscopic classification of icy satellites of saturn — Identification of terrain units on dione and rhea. , 2014, , .		0
101	Thermal inertia of Occator's faculae on Ceres. Planetary and Space Science, 2021, 205, 105285.	1.7	0